



Minerva Access is the Institutional Repository of The University of Melbourne

Author/s:

Whitton, RC;Ayodele, BA;Hitchens, PL;Mackie, EJ

Title:

Subchondral bone microdamage accumulation in distal metacarpus of Thoroughbred racehorses

Date:

2018-11-01

Citation:

Whitton, R. C., Ayodele, B. A., Hitchens, P. L. & Mackie, E. J. (2018). Subchondral bone microdamage accumulation in distal metacarpus of Thoroughbred racehorses. *Equine Veterinary Journal*, 50 (6), pp.766-773. <https://doi.org/10.1111/evj.12948>.

Persistent Link:

<https://hdl.handle.net/11343/283840>

1
2
3
4
5
6
7
8
9
10
11
12
13
14
15
16
17
18
19
20
21
22
23
24
25
26
27
28
29
30
31
32

DR. CHRIS WHITTON (Orcid ID : 0000-0003-0012-4065)

DR. PETA LEE HITCHENS (Orcid ID : 0000-0002-7528-7056)

Article type : General Article

Reference number: EVJ-GA-17-266.R2

Subchondral bone microdamage accumulation in distal metacarpus of Thoroughbred racehorses

R. C. Whitton*, B. A. Ayodele, P. L. Hitchens and E. J. Mackie

Melbourne Veterinary School, Faculty of Veterinary and Agricultural Sciences, University of Melbourne, Melbourne, Australia.

*Corresponding author email: cwhitton@unimelb.edu.au

Keywords: horse; fatigue; osteoarthritis; palmar osteochondral disease; subchondral bone

Summary

Background: Microdamage accumulation leads to subchondral bone injury and/or fracture in racehorses. An understanding of this process is essential for developing strategies for injury prevention.

This is the author manuscript accepted for publication and has undergone full peer review but has not been through the copyediting, typesetting, pagination and proofreading process, which may lead to differences between this version and the [Version of Record](#). Please cite this article as [doi: 10.1111/evj.12948](https://doi.org/10.1111/evj.12948)

This article is protected by copyright. All rights reserved

33 **Objectives:** To quantify subchondral bone microdamage in the third metacarpal bone of
34 Thoroughbred racehorses at different stages of the training cycle.

35 **Study design:** Cross-sectional.

36 **Methods:** Bone blocks from the palmar aspect of the medial condyles of third metacarpal
37 bones from 46 racing Thoroughbred horses undergoing post mortem were examined with
38 micro computed tomography (microCT) to detect calcified microcracks, and light microscopy
39 to quantify bulk stained microcracks. Racing and training histories were obtained for
40 comparison with microdamage data using regression modelling.

41 **Results:** Subchondral bone microcracks were observed in all bones with at least one method.
42 Microdamage grade was greater in older horses, levelling off for horses five years and older
43 (quadratic term $P = 0.01$), and with lower bone material density in the parasagittal groove (P
44 $= 0.02$). Microcrack density was higher in older horses ($P = 0.004$), and with higher bone
45 volume fraction (BV/TV) in the parasagittal groove in horses in training (interaction effect, P
46 $= 0.01$), and lower in horses resting from training ($P = 0.02$).

47 **Main limitations:** Cross-sectional data only. Incomplete detection of microdamage due to
48 the limits of resolution of microCT and lack of three-dimensional imaging with microscopy.
49 Multicollinearity between variables that indicated career progression (e.g. age, number of
50 career starts, duration of training period) was detected.

51 **Conclusions:** Fatigue damage in the distal metacarpal subchondral bone is common in
52 Thoroughbred racehorses undergoing post mortem and appears to accumulate throughout a
53 racing career. Reduced intensity or duration of training and racing and/or increased duration
54 of rest periods may limit microdamage accumulation. Focal subchondral bone sclerosis
55 indicates the presence of microdamage.

56

57 **Introduction**

58 Subchondral bone injury is common in racehorses at sites subjected to high magnitude cyclic
59 loading such as the dorsal aspect of the carpal joints and the palmar aspect of the condyles of
60 the third metacarpal bone in fetlock joints [1; 2]. Subchondral bone injuries occur due to the
61 accumulation of bone fatigue which results in microcracks that develop at the calcified
62 cartilage/hyaline cartilage interface and then propagate into the subchondral bone plate [3-5].
63 Damage can remain confined to the subchondral bone, propagating transversely and resulting
64 in focal subchondral bone injury, or propagate into the trabecular bone to form fractures,
65 some of which may be catastrophic [5; 6].

66

67 Due to the difficulty of detecting microdamage *in vivo* before significant subchondral bone
68 injury develops, and the challenge of treatment once it occurs, minimising such damage in
69 racehorses is highly desirable. An understanding of the factors contributing to the
70 accumulation of subchondral bone microdamage, particularly those that might be modifiable,
71 would inform management strategies more likely to successfully reduce its frequency.
72 Previous studies investigating risk factors for subchondral bone injury have used gross
73 pathology as the outcome rather than the more sensitive quantification of microdamage [2; 7].
74 All methods for detecting microdamage have limitations. Preparation of bone for histological
75 examination can result in the formation of artefactual cracks in the sample. In order to
76 differentiate cracks formed *in vivo* from those induced by sectioning, bone blocks are bulk
77 stained with basic fuchsin before undemineralised sections are cut however this does not
78 prevent cracking from dehydration during the staining process [8; 9]. In addition, a
79 proportion of cracks in equine subchondral bone contain highly mineralised material which is
80 easily observed in undemineralised blocks with backscattered electron microscopy or
81 microCT, however this technique will not allow all cracks to be identified [9; 10].
82 Alternatively, examination of hydrated undemineralised blocks using bright field and
83 differential interference contrast (DIC) microscopy avoids the induction of artefactual
84 cracking via dehydration but not from sectioning [11].

85

86 Microdamage has been quantified in single sections from the lateral and medial condyles of
87 the third metacarpal bone in small numbers of Thoroughbred race horses using a single
88 method (DIC or basic fuchsin bulk staining) [11; 12]. Another study of 38 horses examined
89 one type of microcrack in only two dimensions and found that higher densities of calcified
90 microcracks were associated with increasing age [13]. In the study reported here we examine
91 a new and larger cohort of metacarpi using two methods to detect microdamage in order to
92 mitigate the limitations of each and allow more extensive examination of the parasagittal
93 groove and condyles: microCT to quantify microdamage in three dimensions, and bulk
94 stained sections to quantify all microcracks rather than just those that contained calcified
95 material. Gross injury to the distal metacarpus can affect both lateral and medial aspects with
96 subchondral bone injury more common on the medial condyle and condylar fractures more
97 common in the lateral parasagittal groove and condyle [2; 14]. We examined medial condyles
98 because subchondral bone injuries are more prevalent than condylar fractures [2]; we aimed
99 to investigate the effect of previous training history on the quantity of microdamage present

100 and hypothesised that greater microdamage would be associated with greater racing career
101 duration and greater duration of the current training period at the time of sampling.

102

103 **Materials and methods**

104 The sample size required to estimate the prevalence of microdamage in the population of
105 Victorian racehorses was determined to be at least 34 horses (population size 8,828) for an
106 estimated true prevalence of 90%, with a precision of 10%, and a confidence level of 95%
107 [15; 16].

108

109 The medial condyle and parasagittal groove of a single third metacarpal bone were obtained
110 from 46 racing Thoroughbred horses: 26 in training and 20 resting from training at the time
111 of death. Resting horses were included to determine whether the increased subchondral bone
112 remodelling rates associated with lower levels of activity were associated with microdamage
113 levels [17]. Where the cause of death involved a fetlock injury ($n = 4$) the contralateral
114 metacarpal bone was used otherwise the limb was chosen using a random number table [18].
115 There were 23 left and 23 right forelimbs. The palmar-distal aspect of the metacarpal bones
116 was removed by cutting the bone at 55° to the dorsal plane (dorsodistal-palmaroproximal)
117 through the centre of rotation of the condyles. Samples were stored in 70% ethanol until
118 processing.

119 Racing and training histories were obtained from an official racing database (Racing
120 Australia Limited) and by telephone conversation with trainers. All horses were either in a
121 race preparation (i.e. were racing or training with the intention of racing and had been
122 exercised within one week of sample collection) or, in the case of resting horses, had
123 previously undergone at least one preparation up to galloping speed but had not been
124 exercised for at least one week. Of the 26 horses in training, 15 were male (eight castrated)
125 and 11 female; ages ranged from two to seven years (mean \pm s.d., 4.42 ± 1.72) and each had
126 raced 0 to 59 times (median; 25-75th percentile, 9.0; 1.00-16.0). The duration of the training
127 period at the time of death in these horses was three to 26 weeks (12.0; 8.75-17.0 weeks). Of
128 the 20 resting horses there were 13 males (nine castrated) and seven females resting between
129 one to 14 weeks (4.0; 3.0-8.0 weeks). Ages ranged from two to seven years (3.50 ± 1.40) and
130 each had raced 0 to 54 times (4.0; 0.0-8.0). Additional details of the histories and causes of
131 deaths of horses are available in Supplementary Item 1.

132

133 Palmar osteochondral disease (POD) was graded as previously described [19]. Medial and
134 lateral condyles were separated at the sagittal ridge, then from each medial condyle, bone
135 blocks measuring 10 mm in dorsopalmar width and 10 mm deep at the most distal point of
136 the condyle were cut using a low speed saw (Isomet saw^a). Each block was imaged with
137 micro computed tomography (micro CT) (Scanco 50^b) at 70 kVp, 200 μ A and a voxel size of
138 20 μ m³. Further higher resolution microCT images of the subchondral bone underlying the
139 parasagittal groove and centred at the deepest point of the groove, were also obtained at 70
140 kVp, 200 μ A and a voxel size of 4.4 μ m³. All microCT was acquired in a sagittal plane and
141 then reformatted to enable viewing in multiple planes, with the whole volume examined for
142 microdamage. On microCT images, microcracks were identified as bright linear areas within
143 the bone and are referred to as calcified microcracks in the manuscript (Fig 1). Microdamage
144 in whole condyles was estimated using a grading system based on the number of microcracks
145 and larger fractures observed (Table 1). Calcified microcracks in the higher resolution images
146 of the parasagittal groove were counted. Calcified projections from the calcified cartilage
147 surface into the hyaline cartilage and parasagittal fissures were recorded as present or absent.
148 Bone volume fraction (BV/TV) and bone material density (density of mineralised tissue)
149 were obtained for volumes of interest (VOI) drawn within each acquired volume using the
150 Scanco microCT evaluation algorithms. This approach avoids edge effects and focuses on
151 areas that typically undergo densification in response to loading [14]. The VOI for the lower
152 resolution images was defined by selecting a region measuring 6 mm in dorsopalmar width
153 and 6 mm in distoproximal depth at the most distal point of the condyle and then extending it
154 transversely as far as the sagittal plane through the most proximal point of the condyle (the
155 deepest point of the parasagittal groove; Fig 2A). The VOI defined for the high resolution
156 microCT of the parasagittal groove was derived by selecting the central region (6 mm in
157 dorsopalmar width and 6 mm in distoproximal depth) of each of the 600 sagittal slices
158 centred around the deepest point of the groove (equivalent to 2.64 mm of mediolateral width
159 of the parasagittal groove; Fig 2B).

160
161 For bulk staining, the whole bone blocks prepared for microCT were incubated in 0.2 M NaOH
162 for 48 hours to remove the hyaline cartilage, then stained in 1% basic fuchsin in ascending
163 grades of ethanol (80%, 90% and 100%) under vacuum (20 - 30 mm Hg) for 18 days. Bulk
164 stained samples were embedded in methacrylate resin and oblique dorsal sections (70-90 μ m)
165 were obtained from the middle of the embedded bone blocks using a low speed saw. Bone
166 sections were mounted onto glass slides and cover slipped using Eukitt[®] mounting medium^c.

167 High magnification images of bone sections were obtained by brightfield microscopy (Olympus
168 BX 60^d) and stitched using image analysis software (ImageJ^e). Pre-existing microcracks were
169 identified as oblique linear discontinuities extending from the calcified cartilage into the
170 subchondral bone, and with a surrounding halo of deep basic fuchsin staining [20; 21] (Fig. 3).
171 Microcrack density was calculated on bone sections as previously described [13]. The entire
172 length of the calcified cartilage surface was measured, then stained microcracks that intersected
173 with this interface were counted and expressed as the number of microcracks per millimetre
174 (microcrack density).

175

176 *Data Analysis*

177 Five outcome variables indicating the presence and degree of microdamage were assessed –
178 microdamage, calcified projections, parasagittal fissure, microcrack density (mm), and
179 number of calcified microcracks. To investigate associations between outcome and
180 explanatory variables, we fitted various regression models – an ordered logistic regression for
181 the outcome variable microdamage (graded 0-4); logistic regression for the binary outcomes
182 calcified projections and parasagittal fissure (graded present or absent); and linear regression
183 for the continuous outcome variables microcrack density (mm) and number of calcified
184 microcracks.

185

186 Explanatory variables included categorical terms for limb, sex, training status, presence of
187 catastrophic fracture, and Australian and New Zealand classifications of race distance
188 (whether the horse's longest race in its last five starts was short [≤ 1300 metres], middle
189 [1301-1800 metres], intermediate [1801-2100 metres], long [2101m - 2700 metres], or
190 extended [>2700 metres]). For analysis, we combined middle and intermediate ('middle')
191 and long and extended ('staying'). Horses that had not yet raced were classified as 'unraced'.
192 Continuous terms were also included for age, number of race starts, prize money earned, time
193 in training since last rest period (weeks), time resting since last period of training (weeks),
194 number of races in last 30 days, and time in days between last two starts including the start in
195 which the horse died or was euthanased on a race day. Linear relationships between
196 continuous outcomes and predictors, and between predictors significant in univariable
197 analysis, were assessed by generating scatter plots. Relationships between binary and ordinal
198 outcomes and continuous predictors were assessed using box and whisker plots. Prize money
199 earned and time in days between last two starts were log-transformed for analysis.

200

201 Explanatory variables with unconditional associations significant at the $P < 0.30$ level in
202 univariable models were selected for inclusion in the multivariable models. Models were run
203 with and without microCT variables included. Explanatory variables that were not significant
204 ($P > 0.05$) were removed from the model one at a time, beginning with the least significant.
205 Excluded variables were re-entered into the final model and retained if they changed the
206 estimated regression coefficients by more than 20%. Model diagnostics performed included
207 the link test to identify model specification error, examinations of tolerance (< 0.1) and
208 variance inflation factor ($VIF > 10$) to assess presence of collinearity within the models, and
209 selection of final models based on lower Akaike information criterion (AIC) and Bayesian
210 information criterion (BIC) compared to possible alternate models. Continuous variables
211 were further checked for linearity in the regression models using the Box-Tidwell method.
212 For the ordered logistic regression model for microdamage grade we assessed the
213 proportional odds assumption and fitted a quadratic term for age in the final model.
214 Multicollinearity within the models was detected, particularly between variables that
215 indicated career progression. We chose not to deal with multicollinearity directly within the
216 models, but we further assessed the relationship between age and other continuous variables
217 that were statistically significant in univariable analysis by generating Pearson's pairwise
218 correlation coefficients. Differences between mean age for binary variables (in training,
219 raced) were assessed using Student's t-test. Due to model specification error in the
220 microcrack density model, we assessed two-way interaction terms between the remaining
221 main effects that were significant in multivariable analysis. Assumptions of normality and
222 homogeneity of variance were checked by examining histograms of residuals from the final
223 multivariable models and examining plots of residuals versus predicted values. Odds ratios
224 (OR) and coefficients with their 95% confidence intervals (CIs) are presented for the logistic
225 and linear regression models, respectively. Stata/SE 14.2 for Windows^f was used for
226 statistical analyses.

227

228 **Results**

229 Evidence of gross subchondral bone injury (POD grades 1-3) on the articular surface of
230 medial condyles was observed in 18/46 horses. In all bones examined, subchondral bone
231 microdamage was observed with at least one method, either microCT or light microscopy.
232 Stained microcracks were observed in 43/46 bones with light microscopy. The three bones
233 without stained microcracks were from three 2-year-old horses, two of which had not yet
234 started in a race and one of which had started in one race. In all three of these horses, one or

235 two calcified microcracks were observed on microCT. POD grade was associated with
236 microdamage grade ($P = 0.006$), but not microcrack density ($P = 0.9$) or calcified microcracks
237 ($P = 0.6$). Transverse subchondral bone fractures were observed in three horses two of which
238 had no evidence of gross subchondral bone injury on the articular surface (Fig 4). All were
239 experienced racehorses four to five years old, which had started in a race from five to 25
240 times. Parasagittal fissures were observed on microCT in 14 horses which were 2-7 years of
241 age and had started a race 0-54 times.

242

243 Calcified microcracks were most commonly identified in the parasagittal groove on microCT
244 whereas transverse fractures were identified at different sites across the condyle (Fig 4). Both
245 calcified and bulk stained microcracks were predominantly oriented at 35° to 60° to the
246 articular surface (Figs 1A and 3) as well as slightly oblique to the sagittal plane along the
247 parasagittal groove (Figs 1B and 1C). Calcified projections extending from the calcified
248 cartilage into the hyaline cartilage were observed in 13/46 horses (Fig 5). These structures
249 were always continuous with a calcified microcrack and were most common in the
250 parasagittal groove region. Multiple resorption spaces were observed in a number of the
251 horses resting from training, some of which were immediately adjacent to microcracks (Fig
252 3B).

253

254 Results of univariable analysis are presented in Table 2. In multivariable analysis,
255 microdamage grade was higher in older horses, levelling off for horses five years and older
256 (linear term OR 27.47; 95% CI 3.57, 211.55; $P = 0.001$; quadratic term OR 0.75; 95% CI
257 0.60, 0.93; $P = 0.01$), and in horses with lower bone material density in the parasagittal groove
258 (OR 0.96; 95% CI 0.93, 0.99; $P = 0.020$). Microcrack density was higher in association with
259 older age (Coef. 0.12; 95% CI 0.04, 0.21; $P = 0.004$), and in horses in training compared with
260 those resting from training (Coef. 0.39; 95% CI 0.06, 0.72; $P = 0.02$). In addition, microcrack
261 density was higher with higher BV/TV in the parasagittal groove, but only for horses in
262 training (Fig 6; horses in training main effect, Coef. -3.38; 95% CI -6.29, -0.47; $P = 0.02$;
263 BV/TV in the parasagittal groove main effect, Coef. 1.37; 95% CI -1.73, 4.47; $P = 0.4$;
264 interaction term, Coef. 5.03; 95% CI 1.12, 8.94; $P = 0.01$). Calcified projections were
265 associated with the number of calcified microcracks in the parasagittal groove (OR 1.31; 95%
266 CI 1.11, 1.55; $P = 0.001$). Parasagittal fissures were more common in right forelimbs (OR
267 6.21; 95% CI 1.29, 29.83; $P = 0.02$) and were associated with higher microdamage grade (OR

268 2.24; 95% CI 1.05, 4.78; P = 0.04). Calcified microcracks in the parasagittal groove were not
269 associated with any of the explanatory variables (data not shown).

270

271 Multicollinearity between variables that indicated career progression, such as age, number of
272 starts, frequency of racing, duration of current training period and time resting was detected
273 (see Supplementary Item 2). It was difficult therefore to distinguish which variables were
274 most important biologically and worthy of inclusion in multivariable analysis.

275

276 **Discussion**

277 By detailed quantification of calcified cartilage and subchondral bone microdamage
278 underlying the articular surface of the palmar aspect of the medial metacarpal condyle and
279 parasagittal groove using multiple techniques, we have extended the findings of previous
280 studies showing that microdamage is prevalent in a population of Thoroughbred race horses
281 presenting for post mortem. We found that microdamage becomes more extensive with career
282 progression, in those in race training compared with resting horses, and where there is greater
283 bone volume underlying the parasagittal groove in horses in race training. In addition, gross
284 articular surface damage is not always a good indicator of the amount of microdamage
285 present in the subchondral bone. Other findings such as parasagittal fissures and calcified
286 projections were less commonly observed but were associated with subchondral bone
287 microdamage.

288

289 Microcracks were most prominent in the calcified cartilage and subchondral bone underlying
290 the parasagittal groove extending obliquely from the calcified cartilage surface into the
291 superficial subchondral bone. This position and orientation of microcracks is similar to
292 previous descriptions of subchondral bone at this site, with their oblique orientation
293 consistent with shear failure under compressive loading [5; 12].

294

295 The palmar aspect of the medial metacarpal condyle is subjected to extremely high loads
296 during galloping exercise and is therefore prone to fatigue injury [22]. Fatigue of subchondral
297 bone will accumulate with greater numbers of cycles of loading which equates to greater
298 galloping distance [23]. Therefore, the microdamage resulting from bone fatigue is likely to
299 be more extensive in older more experienced racehorses as we have observed. Three previous
300 studies have related subchondral bone microdamage at this site with age in Thoroughbred
301 racehorses, with one reporting a subjective increase in microdamage associated with age in

302 16 horses and another finding no relationship in 12 horses [11; 12]. A relationship between
303 calcified microcracks and age observed in a previous study did not account for all
304 microcracks [19]. Microcracks in calcified cartilage accumulate in humans with ageing, but
305 in contrast to our findings are rare in young adults and in subchondral bone so it is unlikely
306 that age alone is the cause in horses in training [24; 25]. Grossly visible metacarpal joint
307 surface injury at post mortem has been shown to be associated with total lifetime starts in an
308 older cohort of racehorses, consistent with racing history being more important than age
309 alone [26]. Bone fatigue is also more likely to occur due to the higher loads associated with
310 high speed exercise. It has been observed that subchondral bone microdamage fails to
311 accumulate with exercise at speeds less than or equal to 11 m/s in 18-month-old horses [27].

312
313 Damaged bone can be repaired by remodelling, that is, the removal of bone by osteoclasts
314 and its replacement with new bone by osteoblasts [28] (Fig 3B). It has previously shown that
315 subchondral bone remodelling activity is greatest when horses are resting from training [17].
316 The time frame needed for significant reductions in the microdamage load in horses is
317 unknown, but in rat bone targeted remodelling reduced microdamage by up to 40% within 10
318 days [28]. Although microcrack density across the condyle and parasagittal groove was lower
319 in resting horses than in horses in race training this was not the case for microdamage grade
320 or for calcified microcracks in the parasagittal groove. The lower resolution used to grade
321 microdamage biased this measure towards more severe damage. Such damage might take
322 longer to repair, especially if multicellular units are unable to cross larger disruptions in the
323 bone and cannot access damaged areas. The accumulation of calcified microcracks within the
324 parasagittal groove and the lack of difference in their number between horses in training and
325 those resting suggest that bone repair in this site is less effective than in the condylar
326 subchondral bone. Bone turnover rates showed greater differences between training and
327 resting horses in the lateral condylar subchondral bone than the lateral parasagittal groove
328 [17].

329
330 Previous studies have also found an association between subchondral bone damage and
331 densification of the underlying bone (higher BV/TV) in the parasagittal groove and the
332 condyle [12; 14; 29; 30]. This has prompted proposals that densification results in increased
333 subchondral bone stiffness which promotes initiation of microcracks [12]. However,
334 assuming denser bone is stiffer is flawed as there is no correlation between mechanical
335 properties and bone density in the subchondral bone of the palmar aspect of the metacarpal

336 condyles down to a depth of 6 mm [31]. It is more likely that both densification and
337 microdamage occur independently as a result of high magnitude cyclic loading, i.e.
338 adaptation to the loading environment of the bone through modelling, and damage due to
339 material fatigue [32]. Evidence contradicting a causal relationship between densification and
340 microdamage includes observations that densification of trabecular bone increases its
341 resistance to fatigue damage [33; 34]. Microdamage in human bone has been observed in
342 areas of bone with higher material density (greater mineral content), and it has also been
343 suggested that this is due to a greater brittleness of such bone. However, nanoindentation has
344 shown that these areas are no stiffer than their surrounding bone further demonstrating that it
345 is not possible to make assumptions about bone material properties from imaging [35].
346 Calcified projections from the calcified cartilage surface have been previously described in
347 Thoroughbred racehorses and were associated with cartilage pathology [10; 36]. Based on
348 our observations they appear to arise from an underlying microcrack and therefore are likely
349 part of the pathology associated with fatigue injury along with parasagittal fissures. Similar to
350 our findings, previous work using scanning electron microscopy found calcified projections
351 were not associated with age or training history [36].

352

353 We used two different methods to detect microdamage to offset the limitations of each. Only
354 calcified microcracks and larger fractures are readily identified with microCT however the
355 ability to examine the whole condyle in three dimensions enabled extensive evaluation. Bulk
356 staining permits all microcracks within a section to be visualised but was limited to a single
357 section and therefore may have under-estimated the extent of damage. The mechanism for
358 calcification of microcracks is poorly understood but as this process will take time it is
359 reasonable to expect that calcified microcracks have been present for longer than those that
360 have no evidence of calcification. Therefore, recent microdamage could be overlooked if only
361 calcified microcracks are evaluated. A potential confounder was that resting horses were less
362 likely to have suffered a catastrophic limb injury than those that were in full training at the
363 time of death. However, we included cause of death in our analysis and no confounding
364 effect was observed. Since many of the racing history variables examined were closely
365 correlated and could not be differentiated in terms of individual effect on subchondral bone
366 microdamage, age appeared to be a suitable summary of accumulated training history.

367

368 Our findings suggest that, averaged over time the rate of microdamage accumulation was
369 greater than the rate of microdamage removal by bone repair in horses in this study. This

370 finding is consistent with the accumulation of subchondral bone fatigue injury over a horse's
371 racing career. Two strategies that might limit the accumulation of microdamage are: 1. the
372 provision of adequate periods of rest from training to accelerate microdamage removal or 2.
373 training at a lower intensity to reduce the rate of microdamage accumulation. The length of
374 rest period required to adequately reduce the burden of fatigued subchondral bone is
375 unknown and will depend on bone turnover rates and the volume of damaged bone present at
376 the commencement of the rest period. Returning horses from rest periods results in the
377 additional risk associated with loading subchondral bone that has become more porous in
378 response to a lower loading environment and therefore less resistant to fatigue [37; 38].

379

380 **Conclusion**

381 Fatigue damage in the distal metacarpal subchondral bone is prevalent in Thoroughbred
382 racehorses and appears to accumulate with career progression. Independent of the age of the
383 horse, microdamage levels are lower in resting horses which is consistent with previous work
384 showing higher levels of subchondral bone remodelling during rest periods. Therefore, we
385 recommend reduced intensity and duration of training and racing and/or increased duration of
386 rest periods in order to limit the risk of fatigue injury in racehorses. Although microdamage
387 cannot be detected in live horses with current imaging techniques, the presence of
388 subchondral bone sclerosis, while not necessarily a problem in itself, is suggestive of
389 localised microdamage and should prompt modification of the training regimen.

390

391 **Authors' declaration of interests**

392 No competing interests have been declared.

393

394 **Ethical animal research**

395 The use of animal tissues met the requirements of the University of Melbourne Animal Ethics
396 Committee. Owners gave informed consent for their horses' inclusion in this study.

397

398 **Source of funding**

399 This study was part funded by Racing Victoria Limited and the Victorian State Government
400 which had no role in the study design, the data collection, analysis and interpretation, the
401 writing of the manuscript or in the decision to submit the manuscript for publication.

402

403 **Authorship**

404 R.C. Whitton and E.J. Mackie were responsible for the study concept and design, and
405 obtaining funding. Acquisition of data was by B. Ayodele and R.C. Whitton and analysis by
406 B. Ayodele, P.L. Hitchens and R. C. Whitton. All authors were involved in interpretation of
407 the data, drafting the article, critical revision and final approval.

408

409 **Manufacturers' addresses**

410 ^aBuehler, Lake Bluff, Illinois, USA.

411 ^bScanco Medical AG, Basserdorf, Switzerland.

412 ^cSigma Aldrich, St Louis, Missouri, USA.

413 ^dOlympus, Tokyo, Japan.

414 ^eUS National Institutes of Health, Bethesda, Maryland, USA. <http://imagej.nih.gov/ij/>

415 ^fStataCorp, College Station, Texas, USA.

416

417 **References**

418

419 [1] Dabareiner, R.M., White, N.A. and Sullins, K.E. (1991) Osteolysis of the distal radial
420 and proximal intermediate carpal bones in 57 horses. *Proc. Am. Assoc. Equine Pract.*
421 **31**, 557-561.

422

423 [2] Pinchbeck, G.L., Clegg, P.D., Boyde, A. and Riggs, C.M. (2013) Pathological and
424 clinical features associated with palmar/plantar osteochondral disease of the
425 metacarpo/metatarsophalangeal joint in Thoroughbred racehorses. *Equine Vet. J.* **45**,
426 587-592.

427

428 [3] Radtke, C.L., Danova, N.A., Scollay, M.C., Santschi, E.M., Markel, M.D., Da Costa
429 Gomez, T. and Muir, P. (2003) Macroscopic changes in the distal ends of the third
430 metacarpal and metatarsal bones of Thoroughbred racehorses with condylar fractures.
431 *Am. J. Vet. Res.* **64**, 1110-1116.

432

433 [4] Norrdin, R.W. and Stover, S.M. (2006) Subchondral bone failure in overload
434 arthrosis: a scanning electron microscopic study in horses. *J. Musculo. Neuro.*
435 *Interact.* **6**, 251-257.

436

- 437 [5] Muir, P., Peterson, A.L., Sample, S.J., Scollay, M.C., Markel, M.D. and Kalscheur,
438 V.L. (2008) Exercise-induced metacarpophalangeal joint adaptation in the
439 Thoroughbred racehorse. *J. Anat.* **213**, 706-717.
440
- 441 [6] Riggs, C.M., Whitehouse, G.H. and Boyde, A. (1999) Pathology of the distal
442 condyles of the third metacarpal and third metatarsal bones of the horse. *Equine Vet.*
443 *J.* **31**, 140-148.
444
- 445 [7] Parkin, T.D., Clegg, P.D., French, N.P., Proudman, C.J., Riggs, C.M., Singer, E.R.,
446 Webbon, P.M. and Morgan, K.L. (2005) Risk factors for fatal lateral condylar fracture
447 of the third metacarpus/metatarsus in UK racing. *Equine Vet. J.* **37**, 192-199.
448
- 449 [8] Burr, D.B. and Hooser, M. (1995) Alterations to the en bloc basic fuchsin staining
450 protocol for the demonstration of microdamage produced in vivo. *Bone* **17**, 431-433.
451
- 452 [9] Boyde, A. (2003) The real response of bone to exercise. *J. Anat.* **203**, 173-189.
453
- 454 [10] Laverty, S., Lacourt, M., Gao, C., Henderson, J.E. and Boyde, A. (2015) High density
455 infill in cracks and protrusions from the articular calcified cartilage in osteoarthritis in
456 standardbred horse carpal bones. *Int. J. Mol. Sci.* **16**, 9600-9611.
457
- 458 [11] Turley, S.M., Thambyah, A., Riggs, C.M., Firth, E.C. and Broom, N.D. (2014)
459 Microstructural changes in cartilage and bone related to repetitive overloading in an
460 equine athlete model. *J. Anat.* **224**, 647-658.
461
- 462 [12] Muir, P., McCarthy, J., Radtke, C.L., Markel, M.D., Santschi, E.M., Scollay, M.C.
463 and Kalscheur, V.L. (2006) Role of endochondral ossification of articular cartilage
464 and functional adaptation of the subchondral plate in the development of fatigue
465 microcracking of joints. *Bone* **38**, 342-349.
466
- 467 [13] Bani Hassan, E., Mirams, M., Ghasem-Zadeh, A., Mackie, E.J. and Whitton, R.C.
468 (2016) Role of subchondral bone remodelling in collapse of the articular surface of
469 Thoroughbred racehorses with palmar osteochondral disease. *Equine Vet. J.* **48**, 228-
470 233.

- 471
- 472 [14] Whitton, R.C., Trope, G.D., Ghasem-Zadeh, A., Anderson, G.A., Parkin, T.D.,
473 Mackie, E.J. and Seeman, E. (2010) Third metacarpal condylar fatigue fractures in
474 equine athletes occur within previously modelled subchondral bone. *Bone* **47**, 826-
475 831.
- 476
- 477 [15] Stevenson, M., Nunes, T., Heuer, C., Marchall, J., Sanchez, J., Thornton, R.,
478 Reiczigel, J., Robison-Cox, J., Sebastiani, P., Solymos, P., Yoshida, K. and Firestone,
479 S. *epiR*: An R package for the analysis of epidemiological data. R package version
480 0.9-69.
- 481
- 482 [16] Australian Racing Fact Book (2016): A guide to the racing industry in Australia,
483 2015/16, 2016 edn., Racing Australia Limited, Melbourne, Australia.
- 484
- 485 [17] Holmes, J.M., Mirams, M., Mackie, E.J. and Whitton, R.C. (2014) Thoroughbred
486 horses in race training have lower levels of subchondral bone remodelling in highly
487 loaded regions of the distal metacarpus compared to horses resting from training. *Vet.*
488 *J.* **202**, 443-447.
- 489
- 490 [18] White, J., Yeats, A. and Skipworth, G. (1977) *Tables for statisticians*, University of
491 Queensland Press, St. Lucia, Queensland.
- 492
- 493 [19] Bani Hassan, E., Mirams, M., Mackie, E.J. and Whitton, R.C. (2017) Prevalence of
494 subchondral bone pathological changes in the distal metacarpi/metatarsi of racing
495 Thoroughbred horses. *Aust. Vet. J.* **95**, 362-369.
- 496
- 497 [20] Lee, T.C., Mohsin, S., Taylor, D., Parkesh, R., Gunnlaugsson, T., O'Brien, F.J., Giehl,
498 M. and Gowin, W. (2003) Detecting microdamage in bone. *J. Anat.* **203**, 161-172.
- 499
- 500 [21] Burr, D.B. and Stafford, T. (1990) Validity of the bulk-staining technique to separate
501 artifactual from in vivo bone microdamage. *Clin. Orthop. Relat. Res.* 305-308.
- 502

- 503 [22] Harrison, S.M., Whitton, R.C., Kawcak, C.E., Stover, S.M. and Pandy, M.G. (2014)
504 Evaluation of a subject-specific finite-element model of the equine
505 metacarpophalangeal joint under physiological load. *J. Biomech.* **47**, 65-73.
506
- 507 [23] Martig, S., Lee, P.V., Anderson, G.A. and Whitton, R.C. (2013) Compressive fatigue
508 life of subchondral bone of the metacarpal condyle in thoroughbred racehorses. *Bone*
509 **57**, 392-398.
510
- 511 [24] Mori, S., Harruff, R. and Burr, D.B. (1993) Microcracks in articular calcified cartilage
512 of human femoral heads. *Arch. Pathol. Lab. Med.* **117**, 196-198.
513
- 514 [25] Sokoloff, L. (1993) Microcracks in the calcified layer of articular cartilage. *Arch.*
515 *Pathol. Lab. Med.* **117**, 191-195.
516
- 517 [26] Pinchbeck, G.L., Clegg, P.D., Boyde, A., Barr, E.D. and Riggs, C.M. (2013) Horse-,
518 training- and race-level risk factors for palmar/plantar osteochondral disease in the
519 racing Thoroughbred. *Equine Vet. J.* **45**, 582-586.
520
- 521 [27] Kawcak, C.E., McIlwraith, C.W. and Firth, E.C. (2010) Effects of early exercise on
522 metacarpophalangeal joints in horses. *Am. J. Vet. Res.* **71**, 405-411.
523
- 524 [28] Bentolila, V., Boyce, T.M., Fyhrie, D.P., Drumb, R., Skerry, T.M. and Schaffler,
525 M.B. (1998) Intracortical remodeling in adult rat long bones after fatigue loading.
526 *Bone* **23**, 275-281.
527
- 528 [29] Whitton, R.C., Mirams, M., Mackie, E.J., Anderson, G.A. and Seeman, E. (2013)
529 Exercise-induced inhibition of remodelling is focally offset with fatigue fracture in
530 racehorses. *Osteoporos. Int.* **24**, 2043-2048.
531
- 532 [30] Loughridge, A.B., Hess, A.M., Parkin, T.D. and Kawcak, C.E. (2017) Qualitative
533 assessment of bone density at the distal articulating surface of the third metacarpal in
534 Thoroughbred racehorses with and without condylar fracture. *Equine Vet. J.* **49**, 172-
535 177.
536

- 537 [31] Rubio-Martinez, L.M., Cruz, A.M., Gordon, K. and Hurtig, M.B. (2008) Mechanical
538 properties of subchondral bone in the distal aspect of third metacarpal bones from
539 Thoroughbred racehorses. *Am. J. Vet. Res.* **69**, 1423-1433.
540
- 541 [32] Radin, E.L., Parker, H.G., Pugh, J.W., Steinberg, R.S., Paul, I.L. and Rose, R.M.
542 (1973) Response of joints to impact loading. 3. Relationship between trabecular
543 microfractures and cartilage degeneration. *J. Biomech.* **6**, 51-57.
544
- 545 [33] Rapillard, L., Charlebois, M. and Zysset, P.K. (2006) Compressive fatigue behavior
546 of human vertebral trabecular bone. *J. Biomech.* **39**, 2133-2139.
547
- 548 [34] Fatihhi, S.J., Harun, M.N., Abdul Kadir, M.R., Abdullah, J., Kamarul, T., Ochsner, A.
549 and Syahrom, A. (2015) Uniaxial and Multiaxial Fatigue Life Prediction of the
550 Trabecular Bone Based on Physiological Loading: A Comparative Study. *Ann.*
551 *Biomed. Eng.* **43**, 2487-2502.
552
- 553 [35] Zioupos, P. (2005) In vivo fatigue microcracks in human bone: material properties of
554 the surrounding bone matrix. *Eur. J. Morphol.* **42**, 31-41.
555
- 556 [36] Boyde, A., Riggs, C.M., Bushby, A.J., McDermott, B., Pinchbeck, G.L. and Clegg,
557 P.D. (2011) Cartilage damage involving extrusion of mineralisable matrix from the
558 articular calcified cartilage and subchondral bone. *Eur. Cells Mater.* **21**, 470-478.
559
- 560 [37] Hernandez, C.J., Gupta, A. and Keaveny, T.M. (2006) A biomechanical analysis of
561 the effects of resorption cavities on cancellous bone strength. *J. Bone Miner. Res.* **21**,
562 1248-1255.
563
- 564 [38] Carter, D.R., Hayes, W.C. and Schurman, D.J. (1976) Fatigue life of compact bone--
565 II. Effects of microstructure and density. *J. Biomech.* **9**, 211-218.
566
567
568

569 **Figure legends**

570 **Fig 1:** MicroCT images of subchondral bone underlying the medial parasagittal groove of the
571 third metacarpal bone of a 4-year-old Thoroughbred race horse. A. an oblique dorsal slice
572 through the parasagittal groove into the subchondral bone, B. an oblique transverse slice
573 aligned with articular surface of the parasagittal groove, C. a three-dimensional
574 reconstruction of bone from the parasagittal groove. Numerous calcified microcracks are
575 observed in the calcified cartilage and extending into the subchondral bone obliquely oriented
576 to the articular surface and to the parasagittal groove (arrowheads in A). Scale bars = 1 mm.

577

578 **Fig 2:** MicroCT images of a third metacarpal bone illustrating VOIs for estimation of BV/TV
579 and material density. A. The image on the left is an oblique dorsal view showing the
580 lateromedial extent of the low resolution VOI (VOI 1); the dotted line indicates the plane of
581 the sagittal view shown on the right, which demonstrates the dorsopalmar extent of the VOI.
582 B. Oblique dorsal view showing the lateromedial extent of the high resolution VOI (VOI 2),
583 which was comprised of 600 sagittal slices similar to those shown in the right image of panel
584 A.

585

586 **Fig 3:** Two photomicrographs of oblique dorsal sections bulk stained with basic fuchsin: A
587 through the parasagittal groove and condylar articular surface of the third metacarpal bone of
588 a 4-year-old Thoroughbred racehorse in race training with multiple stained microcracks
589 extending obliquely from the tidemark into the subchondral bone (arrow heads) , scale bar =
590 1 mm, and B through the parasagittal groove of the third metacarpal bone of a 5-year-old
591 Thoroughbred racehorse that had been resting for 4 weeks. Stained microcrack (black arrows)
592 with a resorption space forming at the tip of the microcrack (white arrows), scale bar = 100
593 μm .

594 **Fig 4:** Oblique dorsal microCT image of subchondral bone underlying the medial condyle
595 and parasagittal groove of the third metacarpal bone of a 5-year-old Thoroughbred racehorse.
596 A transverse fracture is observed extending lateromedially through the condylar subchondral
597 bone. Scale bar = 1 mm.

598

599 **Fig 5:** Dorsal (A) and sagittal (B) microCT image of subchondral bone underlying the
600 parasagittal groove of the third metacarpal bone of a 4-year-old Thoroughbred racehorse.

601 Calcified projections (arrows) are observed extending from the calcified cartilage surface into
 602 the hyaline cartilage. Scale bar = 1 mm.

603

604 **Fig 6:** Relationship between microcrack density (mm) and bone volume fraction (BV/TV) of
 605 the parasagittal groove for horses in training (circles) and those not in training (triangles)
 606 (interaction effect, $P = 0.01$). Marginal effects with 95% confidence intervals are presented.

607

608

609 **Table 1:** Grading system for microCT images.

610

Finding	Grade	Description
Microdamage	0	No microcracks
	1	One or two microcracks
	2	Three to ten microcracks
	3	More than ten microcracks
	4	Fracture

611 **Table 2:** Univariable associations between subchondral bone microdamage in medial condyles of third metacarpal bones and explanatory
 612 variables, from 46 Thoroughbred racehorses. Explanatory variables of $P < 0.30$ were considered for inclusion in logistic regression models
 613 reporting Odds ratios (ORs), and linear regression models reporting coefficients (Coef.) multivariable models. Calcified microcracks in the
 614 parasagittal groove were not associated with any of the explanatory variables (data not shown).
 615

	Microdamage grade		Microcrack density (mm)		Calcified Projections		Parasagittal fissure	
	OR (95% CI)	<i>P</i> -value	Coef. (95% CI)	<i>P</i> -value	OR (95% CI)	<i>P</i> -value	OR (95% CI)	<i>P</i> -value
Age	1.87 (1.30,2.67)	0.001	0.22 (0.12,0.32)	<0.001	1.43 (0.97,2.13)	0.07	1.11 (0.76,1.63)	0.595
Sex								
Male (entire)	Ref		Ref		Ref		Ref	
Male (gelding)	2.01 (0.52,7.75)	0.311	0.17 (-0.34,0.68)	0.514	11.25 (1.17,108.41)	0.04	0.95 (0.20,4.64)	0.954
Female	0.45 (0.11,1.77)	0.254	0.01 (-0.49,0.52)	0.957	5.00 (0.51,48.75)	0.2	0.50 (0.10,2.62)	0.412
Right vs. Left limb	1.81 (0.63,5.19)	0.269	0.21 (-0.18,0.59)	0.288	1.47 (0.43,4.98)	0.5	6.11 (1.41,26.41)	0.015
In training	1.24 (0.44,3.55)	0.684	0.56 (0.21,0.92)	0.002	0.67 (0.20,2.26)	0.5	1.04 (0.29,3.69)	0.955
Duration of training period (weeks)	1.03 (0.96,1.10)	0.377	0.05 (0.02,0.07)	<0.001	0.99 (0.91,1.07)	0.75	0.98 (0.91,1.07)	0.710
Time resting	0.92 (0.80,1.06)	0.237	-0.06 (-0.11,-0.01)	0.014	0.95 (0.80,1.14)	0.6	1.00 (0.84,1.18)	0.967
Raced	7.84 (2.11,29.19)	0.002	0.32 (-0.10,0.74)	0.140	2.17 (0.50,9.40)	0.3	1.67 (0.38,7.32)	0.499
Starts	1.06 (1.02,1.11)	0.002	0.02 (0.01,0.03)	0.002	1.02 (0.98,1.07)	0.3	1.01 (0.97,1.06)	0.520
Time between last two starts (log)	0.71 (0.28,1.82)	0.479	-0.04 (-0.31,0.22)	0.756	4.11 (1.00,16.90)	0.05	2.28 (0.79,6.59)	0.128
Races in last 30 days	1.65 (1.02,2.67)	0.040	0.31 (0.14,0.48)	<0.001	0.98 (0.55,1.73)	0.9	0.88 (0.46,1.67)	0.691
Longest distance last 5 starts								
0 (unraced)	Ref		Ref		Ref		Ref	
1000-1300m	4.35 (0.92,20.63)	0.064	0.02 (-0.50,0.53)	0.946	1.43 (0.22,9.26)	0.7	1.43 (0.22,9.26)	0.708

1301-2100m	11.23 (2.36,53.43)	0.002	0.27 (-0.20,0.73)	0.256	2.92 (0.57,15.05)	0.2	1.67 (0.31,8.93)	0.551
>2100m	10.63 (2.01,56.08)	0.005	0.79 (0.24,1.34)	0.005	2.00 (0.29,13.74)	0.5	2.00 (0.29,13.74)	0.481
Prizemoney (log)	1.51 (1.06, 2.13)	0.021	0.08 (-0.01,0.18)	0.097	1.08 (0.77,1.52)	0.7	1.09 (0.76,1.56)	0.628
Prizemoney								
No prizemoney (unraced)	Ref		Ref		Ref		Ref	
<100k	5.89 (1.51,22.94)	0.011	0.23 (-0.22,0.67)	0.313	1.78 (0.38,8.37)	0.5	1.46 (0.30,6.98)	0.637
≥100k	17.82 (3.27,97.03)	0.001	0.52 (-0.02,1.06)	0.058	3.33 (0.56,19.95)	0.2	2.22 (0.36,13.54)	0.386
Fracture	1.06 (0.36,3.14)	0.920	0.33 (-0.05,0.73)	0.086	0.54 (0.15,1.96)	0.3	1.18 (0.32,4.37)	0.797
BV/TV condyle	2.04 (0.00,>18k)	0.878	3.99 (0.82,7.16)	0.014	0.00 (0.00,166.89)	0.3	186.46 (0.00, >23m)	0.384
Parasagittal BV/TV	1437.9 (0.47,>4m)	0.076	5.86 (3.53,8.19)	<0.001	30.37 (0.00,>322k)	0.5	42.73 (0.00,>661k)	0.446
Parasagittal Material density	0.97 (0.95,1.00)	0.063	0.00 (-0.01,0.01)	0.966	0.98 (0.95,1.01)	0.2	0.99 (0.96,1.02)	0.574
Calcified microcracks	1.12 (1.00,1.24)	0.045	0.03 (-0.01,0.07)	0.193251	1.31 (1.11,1.55)	0.001	1.16 (1.01,1.33)	0.031
Microcrack density (mm)	3.97 (1.63,9.66)	0.002	n/a		1.21 (0.49,3.00)	0.7	2.34 (0.89,6.15)	0.086
Microdamage grade	n/a		0.25 (0.09,0.41)	0.002	1.49 (0.83,2.65)	0.2	2.18 (1.09,4.34)	0.027

616 Note: The final models were correctly specified according to the link test; the proportional odds assumption was satisfied for the ordered logistic regression model.

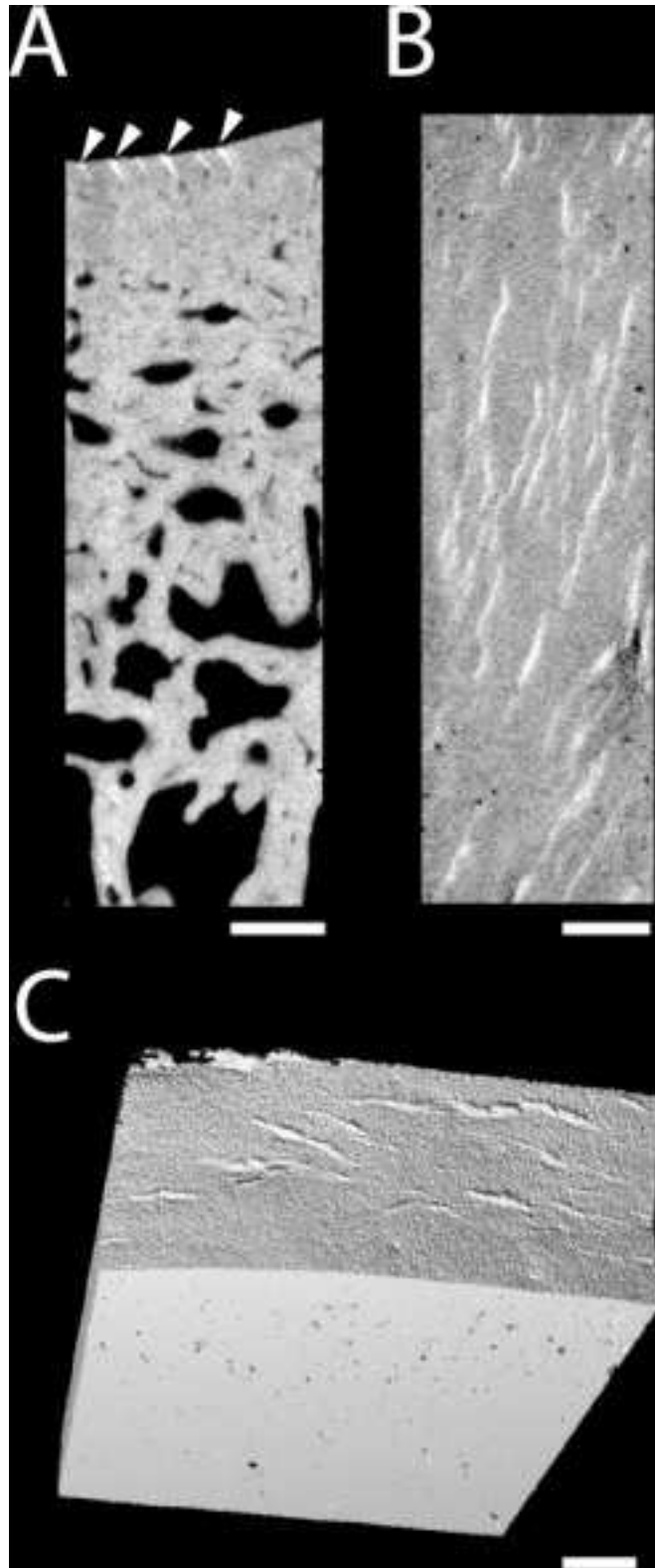
617

618

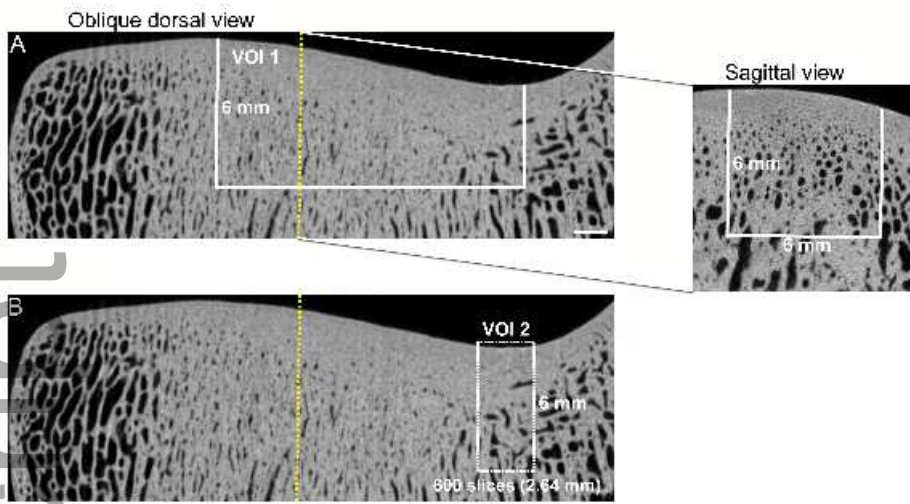
619 **Supporting Information**

620 **Supplementary Item 1:** Additional clinical and racing history.

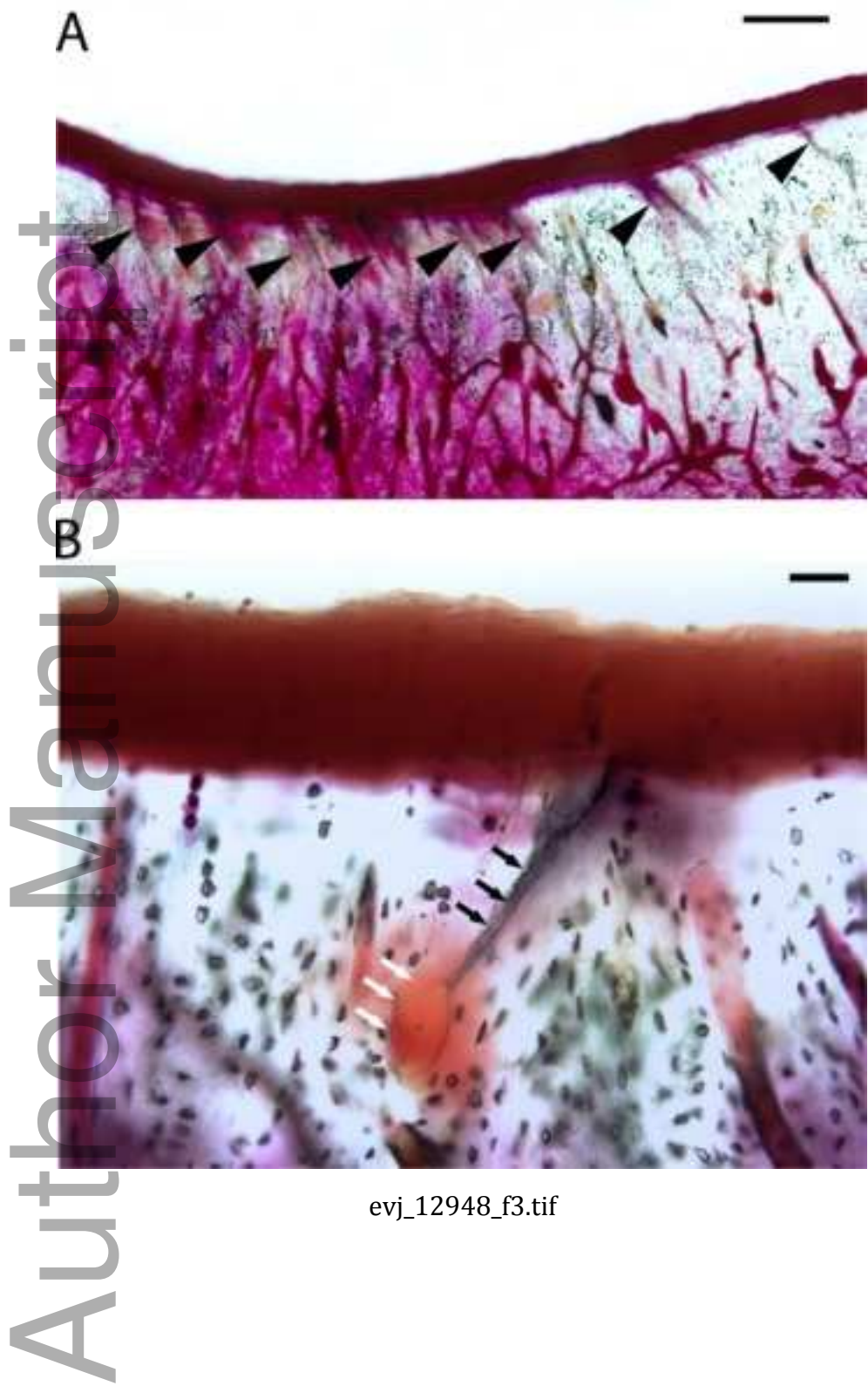
621 **Supplementary Item 2:** Correlations between variables associated with career progression.

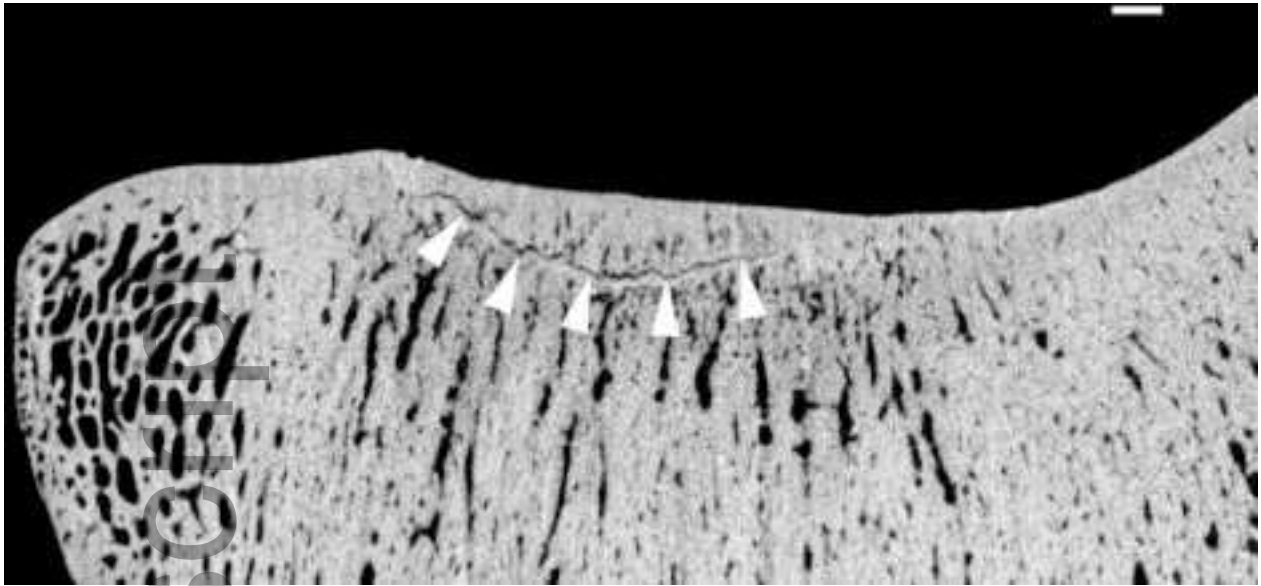


evj_12948_f1.tif



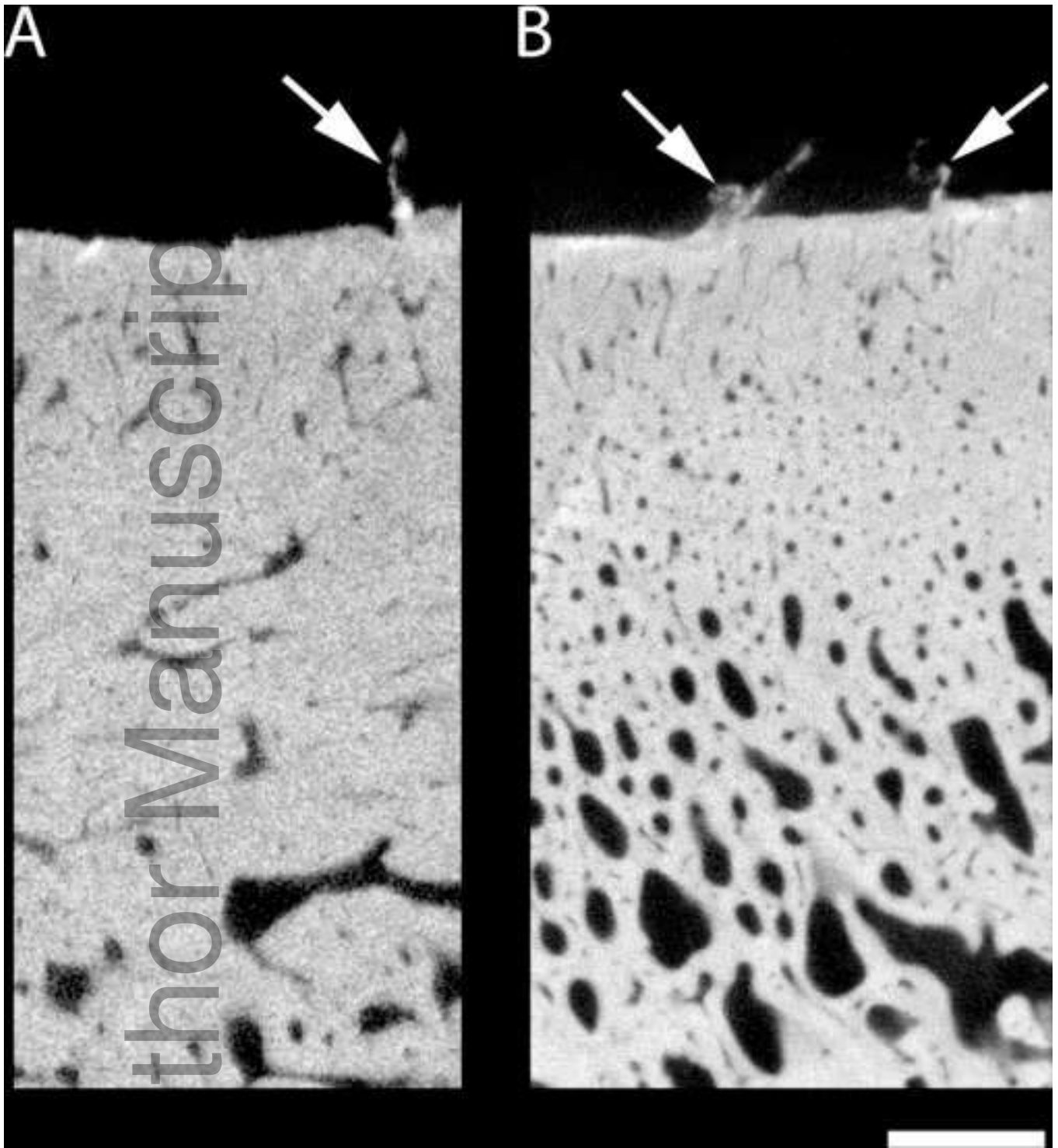
evj_12948_f2.tif





evj_12948_f4.tif

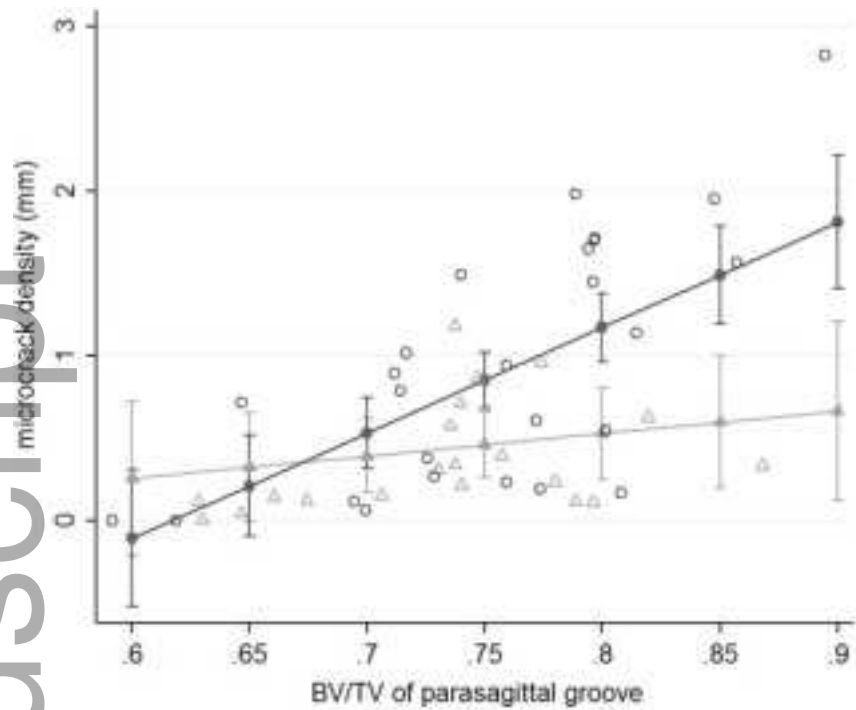
Author Manuscript



Author Manuscript

A

evj_12948_f5.tif



evj_12948_f6.tif